DOI: 10.1021/ma900375g

Macromolecules
ARTICLE

Glass Transition Behavior of Single-Walled Carbon Nanotube−Polystyrene Composites

Brian P. Grady,*[,†,‡] Abhijit Paul,[§] Jonathan E. Peters,[†,‡] and Warren T. Ford[§]

[†]*Carbon Nanotube Technology Center (CaNTeC) and* [‡]*School of Chemical, Biological, and Materials Engineering, University of Oklahoma Norman, Oklahoma 73019, and* [§]*Department of Chemistry, Oklahoma State University, Stillwater, Oklahoma 74078*

Received February 18, 2009; Revised Manuscript Received July 10, 2009

ABSTRACT: A variety of measurements using a differential scanning calorimeter were used to probe how single-walled carbon nanotubes (SWCNTs) affect polymer dynamics associated with the glass transition. Tubes were dispersed in *N*,*N*-dimethylformamide containing dissolved polystyrene, and precipitation was quickly forced by the addition to large amounts of water. The percolation threshold was found to be less than 0.5 wt %, indicating good dispersion of the tubes. The glass transition temperature (T_g) increased at low nanotube fractions to a constant value about 6−7 °C higher than the T_g of pure polystyrene, and did not change further as the nanotube amount changed from 1 to 30 wt %. The heat capacity change at the glass transition decreased with increasing nanotube concentration, except at very high SWCNT contents (> 10 wt %), where the heat capacity change began to increase. The decrease of heat capacity at low nanotube contents indicates that a fraction of the polymer is made immobile via the addition of SWCNTs; while the large increase at high contents suggests that nanotubes are participating in the molecular motion that is the glass transition. The relaxation rate as determined by the change in limiting fictive temperature with annealing time showed the same qualitative behavior as the glass transition, a decrease in polymer mobility at very low nanotube fractions followed by a constant value. Surprisingly, one measure of the activation energy increased at low nanotube contents (< 0.5 wt %) and dropped at high nanotube contents to an energy that looks to be slightly higher than that for pure polystyrene. In other words, in the region where the formation of a continuous network occurs the activation energy is highest.

Introduction

Single-walled carbon nanotubes (SWCNTs) are one of a number of nanofillers currently being considered for use in polymer composites. Nanofillers can be divided into three geometric types: one-dimensional, two-dimensional, or three-dimensional. A one-dimensional nanofiller has one dimension with nanometer length-scale; an important commercial example used in polymers is montmorillonite nanoclays. A three-dimensional nanofiller has three dimensions with nanoscale dimensions; an important commercial example used in polymers is alumina nanoparticles. SWCNTs are an example of a two-dimensional nanofiller; only the length of the tube is of non-nanoscale dimension. In many cases, the geometry is an important reason why a nanofiller is considered for a given application; for example gas barriers in nanoclay-filled materials and electrical conductivity at low volume fractions in nanotube-filled materials. The work described in this paper explores how a two-dimensional nanofiller changes polymer dynamics around the glass transition.

Fundamental studies of how a surface affects the chain dynamics of polymers have been a very fertile field of investigation. The influence of a solid interface on the glass transition (T_g) behavior of a polymer was first investigated by using thin films cast on flat surfaces.[1−4] More recently, polymers containing particles with significant surface area/volume ratios, i.e. nanofilled materials,[5] have been used. In the latter case, simple geometric arguments can be used to show that the average distance between a polymer and a surface is in the tens of nanometer range depending on dispersion and filler loading, and hence, if dispersion is good, then using nanocomposites to investigate how a solid surface affects the T_g is reasonable. Both one-[6−8] and three-dimensional nanofillers[9−11] have been investigated in significant detail; however a similar investigation of a two-dimensional nanofiller has not been reported to our knowledge, with one exception. Recently, Zhong et al.[12] reported investigations of the dependence of the relaxation times on nanofiller loading by calculating the activation energy of enthalpy relaxation and the width of the relaxation time distribution using thermal analysis on graphite nanofibers. However the amount of filler in the polymer was in all cases less than 1 wt % and the diameters of these nanofibers were not given. The diameter of the nanofibers studied by Zhong et al. seems to be in the tens of nanometer range, if not the hundred of nanometer range. If individually dispersed, the fillers used in the present study have diameters ∼1 nm.

The effect of a solid surface on polymer dynamics depends on the nature of the interaction between the polymer and the surface. In the case of a favorable interaction between the surface and the polymer, three effects might be observed in a normal differential scanning calorimetry (DSC) heating scan of an amorphous polymer around the T_g: (1) an increase in the glass transition temperature; (2) a change in the temperature range over which the glass transition occurs; (3) a reduction in the heat capacity increase at T_g. The latter represents the case where the dynamics have been altered for a fraction of the material to such an extent so as to cause a separation between regions of the polymer in a dynamic sense.[13] This separation could cause a noticeable second glass transition at a higher temperature, or could cause no noticeable second glass transition if the second glass transition is above the degradation temperature of the polymer.

Many studies involving SWCNT-polymer composites have shown an increase[14,15] as well as broadening[15,16] in T_g, although

*Corresponding author. E-mail: bpgrady@ou.edu.

 Published on Web 07/27/2009

by no means are such behaviors universally observed in SWCNT-polymer composites.[17,18] Only two studies, one using covalently bonded nanotubes and a segmented polyurethane[19] and the other poly(L-lactide),[20] have reported a decrease in heat capacity jump at the glass transition for nanotube-based composites. In this study, a number of approaches using thermal analysis, more fully described in the Experimental section, are used to measure polymer dynamics around the glass transition. None of these methods have been used on nanocomposites filled with two-dimensional nanofillers except for the paper by Zhong et al.[12] using graphitic nanofibers described earlier.

Experimental Section

Materials and Sample Preparation Method. A solution of polystyrene (Aldrich; $M_w = 210\,000$ g/mol; polydispersity = 3.0) in dimethyl formamide (DMF) and a bath-sonicated dispersion in DMF of lightly oxidized HiPCo SWCNTs (lot #P0340) provided by Carbon Nanotechnologies were combined, sonicated, and added slowly to water to precipitate the composite, and then dried.[21] Composites were placed in DSC pans in the form of a thin layer of powder as equally distributed as possible, and a 15-min premelting step at 180 °C was used to produce good sample−pan contact. Polystyrene was used as received; mechanical forces were used to reduce pellet size but the average particle size was significantly larger than for the composite samples. T_g was found to be a sensitive measure of whether sample−pan contact was sufficient; in some cases 1−2 runs were required before the T_g reached a limiting constant value. In all cases, samples sizes were between 2 and 4 mg in order to minimize thermal gradients; in the latter case, if the sample forms a thin film (which these samples almost certainly do not), this corresponds to a sample thickness less than 0.15 mm thick.

Low nanotubes content samples could easily be molded into very small thin films. Electrical conductivities were tested by the two point probe method with a specially constructed resistivity chamber, calibrated by a Keithley 610C electrometer. The lower limit of conductivities that could be measured with this equipment was approximately 5×10^{-17} S/cm.

DSC Methods. Indium, tin, and biphenyl were used for temperature calibration. Sapphire was used as the enthalpy calibrant because it gave a better value for the heat capacity of polystyrene.[22] Both hermetically sealed and normal crimped pans were used with sapphire and, within experimental error, the two agreed. Calibration was made at whatever heating or cooling rate required for the experiment of interest. Glass transition measurements made during heating were used to monitor sample degradation; small drifts (1−2 °C) upward in T_g were taken as indications that the sample was degrading. In addition, upward curvature in the high temperature heat capacity was also taken as evidence of sample degradation. Samples were remade if any evidence of either phenomena occurred. All DSC samples had to be remade at least once.

Glass Transition Temperature Measurement. Glass transition temperatures (T_g) and heat capacity jump (ΔC_p) at the glass transition were measured by DSC using a 10 °C/min temperature ramp without modulation after a 60 °C/min cooling from a fully melted sample. Standard procedures were used, including thin samples and normal crimped aluminum pans. The heat capacity jump was determined by the difference in y-values of the two intersection points between the dotted lines shown in Figure 1 and a tangent line (not shown) drawn at the inflection point of the heat capacity change at the glass transition. The glass transition temperature was determined as average of the x-values of the two intersection points. Measurements during heating were made multiple times over many months using different samples; the largest source of error was differences due to different samples.

The glass transition temperature was also measured during cooling at a rate of 10 °C/min from a fully melted sample. For a given nanotube content, the same sample was used for all cooling measurements. Simon et al. discusses the advantages from a thermodynamic perspective of measuring the glass transition by cooling.[23] Our position is that measuring during heating is perfectly appropriate if cooling rates are fast enough to prevent enthalpy relaxation being present during heating because any undershoot can be comfortably ignored. A cooling rate of 60 °C/min and a heating rate of 10 °C/min met this requirement in all cases. However, to confirm the effects described in the next section it was deemed prudent to make T_g measurements under cooling as well. The same procedure shown in Figure 1 was used to calculate T_g and ΔC_p. Our group was only able to obtain one standard appropriate for calibrating temperature upon cooling, BCH-52,[24] so it was assumed that the offset (actual temperature-measured temperature with no calibration factor applied) was consistent across the entire temperature range. This assumption is likely not a good one since this offset was not constant for calibration done in heating; in heating the offset for biphenyl was about 0.2 °C while that for tin was almost 2 °C.

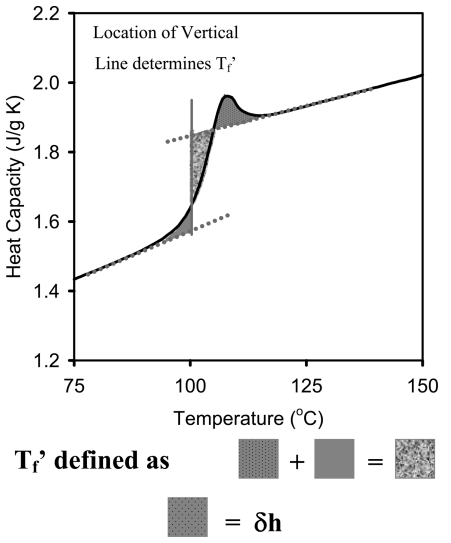

Figure 1. Equal area method used to determine limiting fictive temperature ($T_{f\,spm}$') as well as to show determination of recovered enthalpy (δh).

Relaxation Rate and Fictive Temperature. In one set of experiments, samples were annealed for a certain amount of time t_a and then the heat capacity measured after a rapid cool. In these experiments, T_g − 20 °C was used as the annealing temperature and samples were quickly cooled and reheated using a 10 °C/min heating rate. The relaxation rate was measured according to[6]

$$R_E = \frac{-d(T_f - T_a)}{d(\log t_a)} \quad (1)$$

where R_E is the relaxation rate and T_f is the fictive temperature. The fictive temperature concept was defined by Tool[25] to describe the thermodynamic state of glasses. Essentially, the structural relaxation that occurs in glasses must be described by a relaxation time that depends on temperature as well as the instantaneous glass structure (which in turn depends on the thermal history of the sample). The fictive temperature is essentially a temperature that accounts for this structure. The fictive temperature is calculated using the "equal area method"[26] upon heating scans as also shown in Figure 1.

Activation Energy from the Cooling Rate Dependence of the Glass Transition Temperature. The activation energy, Δh^*, is calculated from the Tool−Narayanaswamy−Moynihan equation,[25−27] which describes the dependence of relaxation time on both the temperature and structure. Moynihan et al. proposed a

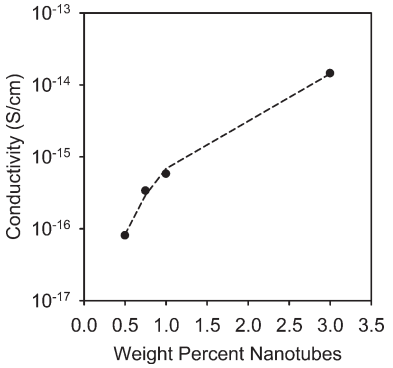

Figure 2. Conductivity as a function of nanotube content. Dotted line represents best-fit according to eq 4.

method to measure the activation energy using the cooling rate dependence of the glass transition.[28,29] This method involves measuring the change in glass transition temperature as a function of cooling rate q; where T_g is measured during heating with the heating rate equal to the cooling rate. The activation energy can be calculated according to the formula

$$\Delta h^* = -R\frac{\mathrm{d}[\ln(q)]}{\mathrm{d}(1/T_g)} \tag{2}$$

where R is ideal gas constant. Rates between 10 and 1.25 °C/min were used with factor of 2 steps between individual rates. To adjust for the fact that the calibration constants for temperature depend on the heating rate, the DSC was recalibrated at the given heating rate for each measurement.

Activation Energy from the Cooling Rate Dependence of the Limiting Fictive Temperature. Another method to calculate the activation energy is from the cooling rate dependence of the limiting fictive temperature, T_f'. In this method, Δh^* is calculated from the following:

$$\frac{\Delta h^*}{R} = \frac{-\mathrm{d}[\ln(q)]}{\mathrm{d}(1/T_f')} \tag{3}$$

The experimental procedure consists of cooling the sample at some rate q (°C/min) and then measuring the fictive temperature, in this case the limiting fictive temperature T_f', during a heating scan (10 °C/min was used). With no aging time between heating and cooling, the fictive temperature is termed the limiting fictive temperature. This same expression can be modified slightly to determine the fragility index;[30] both parameters fundamentally describe the same phenomena. T_f' was calculated as described previously.

Results and Discussion

The plot of electrical conductivity vs weight fraction (Figure 2) has the expected percolation behavior and the following equation was used to fit the data:

$$\sigma = A(m - m_{c\sigma})^{\beta\sigma} \tag{4}$$

where σ is electrical conductivity, m is SWNTs mass fraction, $m_{c\sigma}$ is the electrical percolation threshold, β_σ is the critical exponent, and A is a scaling constant. The logarithm of this equation was used to fit the data; however a direct nonlinear least-squares procedure was not able to find the global minimum unless the initial guesses were extremely close to the final answer. Instead, values of $m_{c\sigma}$ were fixed at 0.0005 (0.05%) intervals and the best fit A and β_σ were determined for a given $m_{c\sigma}$. The value of $m_{c\sigma}$ and the associated best fit A and β_σ that had the smallest sum of the square of the errors for all ($m_{c\sigma}$, A, β_σ) was determined as the best-fit. The values were $m_{c\sigma}$ as 0.10%, while β_σ was 2.6. The former value indicates that the dispersion was good, while the latter value is consistent with what others have found for similar dispersion methods.[31] The plateau conductivity is also quite low, indicating that the tubes were of low quality with respect to electrical conductivity.

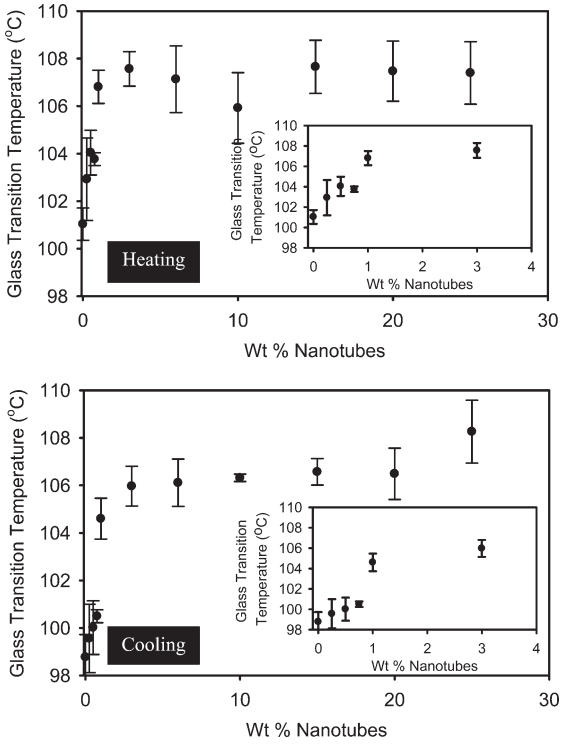

Figure 3. Glass transition temperature as a function of nanotube content. For heating, data was collected at 10 °C/min heating rate immediately after a 60 °C/min cool to −50 °C. For cooling, data was collected at a 10 °C/min cooling rate. Error bars represent errors calculated from duplicate measurements.

The glass transition temperature increases slightly at low nanotube contents, and then reaches a plateau as shown in Figure 3 for both heating and cooling. Some of the slight difference in values between heating and cooling could be a result of temperature calibration errors in cooling; however some offset is also expected due to the different measurement protocols. A recent paper using a latex dispersion method showed that for a material having a very low average molecular weight, T_g increased from 90 to 107 °C as the nanotube content increased. T_gs were roughly identical only above 2 wt % SWCNT content.[32] A rather large increase in T_g was also found for polystyrene melt-mixed with MWCNTs where the starting T_g was also very low;[33] a low T_g is indicative of a very low average molecular weight polystyrene. For the latex-mixed material with a starting T_g that has a more typical value (~100 °C), there was a small decrease in T_g with added nanotubes, attributed to surfactant plasticization. When a small amount of low molecular weight material was added, the T_g did show a slight increase.[32] A study using a similar solution dispersion method as what was done for this paper showed an increase in T_g below 1% tubes with a plateau in T_g being reached that persisted to 3% tubes. This result is qualitatively similar to what is shown in Figure 3. However the magnitude of the increase was 3 °C,[34] which is about half the increase in T_g found here. The authors also noted a substantial broadening of the transition; such broadening was not found in this current study. Grafting of polystyrene onto MWCNTs led to an extremely large increase in glass transition temperature; an

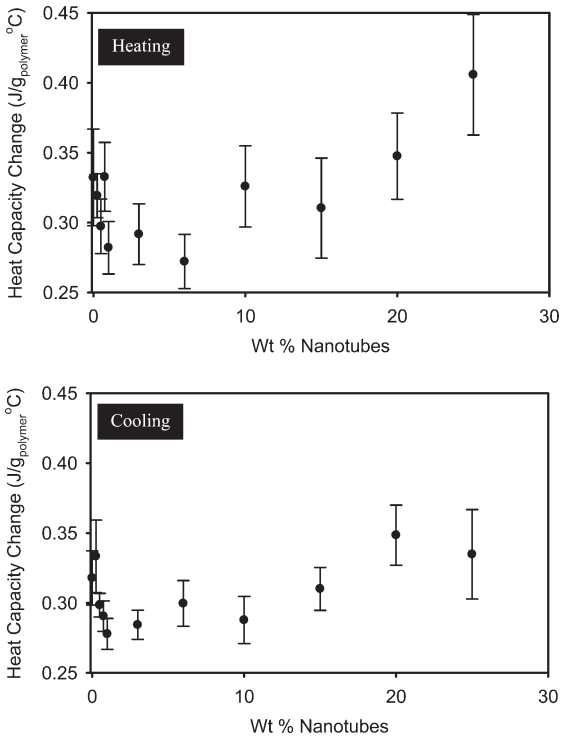

Figure 4. Change in heat capacity at glass transition at the same conditions described in Figure 3. Error bars represent errors calculated from duplicate measurements.

increase of ~35 °C at 40 wt % nanotubes.[35] Taken together, the results show that the change in T_g depends on the interaction of the polystyrene with the nanotube surface, which is dependent on nanotube type, purification procedures and modification procedures (if any) will have a great deal of impact on the observed behavior.

The magnitude of ΔC_p is proportional to the amount of material participating in the glass transition. Figure 4 shows the change in the specific heat capacities for the samples in this study. The increase in T_g coupled with the lowering of the heat capacity jump at low added nanotube contents strongly suggest that some polymer is immobilized by the introduction of nanotubes, i.e., a polymer within the immediate vicinity of a nanotube interface. The plateau in heat capacity at ~1% nanotube content is a bit surprising, since one would expect the fraction of polymer within a certain distance of nanotube to increase as the nanotube fraction increases. However, dispersion changes as well as the possibility that the average end-to-end distance of the polystyrene may change with a change in nanotube content make such a result feasible. Also, the constancy of T_g begins at roughly the same nanotube fraction as the constancy begins for the heat capacity change, i.e. 1% nanotubes.

The increase of ΔC_p at very high nanotube contents is interesting and novel. One explanation is that nanotubes are changing dynamics as a polymer goes through its T_g. It is been reported that, for two-dimensional nanofillers, melt annealing or relaxation after shear can cause a substantial change in electrical conductivity, which indicates that there must be some movement of the filler to increase filler connectiveness.[36−41] If such movement can occur in the melt, it is certainly possible that such movement can occur at the glass transition. However, this type of movement has typically been attributed, at least in part, to some sort of cluster formation and aggregation. If the structural change is due only to cluster formation and aggregation then the two phenomena, i.e. the change in electrical conductivity with time and increase in heat capacity jump, are not related.

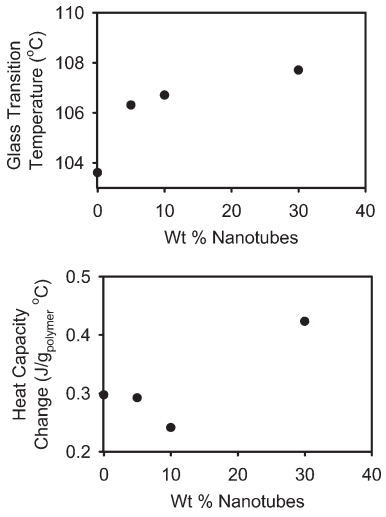

Figure 5. Same plots as Figure 3 and Figure 4 except for samples prepared from surfactant-assisted dispersion of nanotubes with dispersed latex (see text for further description of samples).

Further, clustering during annealing is not at all limited to two-dimensional nanofillers; other fillers have shown similar phenomena.[42−44] In other words, if nanotube movement involves only center-of-mass translation or rigid-body rotation, then it is difficult to understand why this motion would contribute to a change in the heat capacity, since the time and length scales of such motions should be very long. However, if filler movement occurs on a tens of nanometer scale and involves only a portion of a tube, which is certainly possible for individually dispersed SWCNTs, then a jump in heat capacity is possible.

Another possible explanation for the change in heat capacity at high nanotube contents is that configuration changes of the polymer cause a larger change in heat capacity difference between the liquid and the bulk. In bulk polyacrylonitrile[45] and in solution,[46] it has been shown that nanotubes can alter single-chain configurations for chains near tubes. Perhaps at high enough nanotube contents enough configurations can be altered to cause an increase in heat capacity; however it is hard to understand why there would also not be a change in glass transition temperature. In heating, only the ΔC_p at 25% nanotubes is statistically above that for pure polystyrene while in cooling no values are statistically above those for pure polystyrene. Hence, the increase could be formerly immobilized polystyrene being decoupled from the tubes; although this explanation is unlikely since the glass transition temperature behavior is not consistent with this phenomena. Further, what would cause such a decoupling? An interesting question, which our laboratory plans to explore, is whether the increase in heat capacity at high nanotube contents also occurs for MWCNT-filled materials; we are not aware of any studies involving nanofillers where an increase in the heat capacity change at the glass transition with added filler content was presented.

Figure 5 shows T_g and ΔC_p for SWCNT-polystyrene composites made using a latex-dispersion method and CoMoCAT SWCNTs. These materials contain substantial amounts of surfactant (roughly a 1:1 correspondence between surfactant amount and nanotube amount); details concerning sample preparation etc. are given in a previous publication.[47] T_g and ΔC_p changes qualitatively match what was found for the solution-mixed materials. This graph demonstrates that the phenomenon of increasing ΔC_p at high nanotube contents is very possibly a general phenomenon for SWCNT composites.

A number of different measures of glass transition temperature behavior are presented in this paper to build an overall picture of

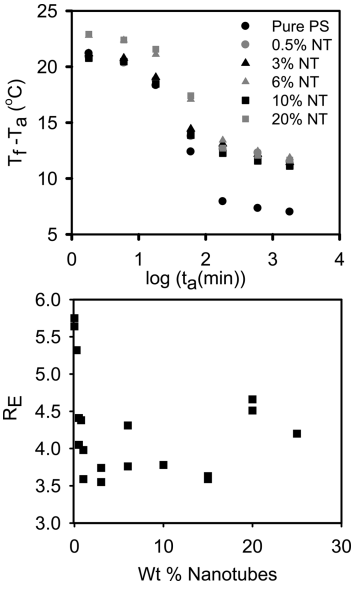

Figure 6. Relaxation rate as calculated from the change in fictive temperature with annealing time (t_a); units of R_E are consistent with top plot. Data was gathered from a 10 °C/min heating scan performed after annealing at $T_g - 20$ °C. (Duplicates are shown rather than error bars because of the large machine time required for the minimum 3−5 sets of runs required for error bars).

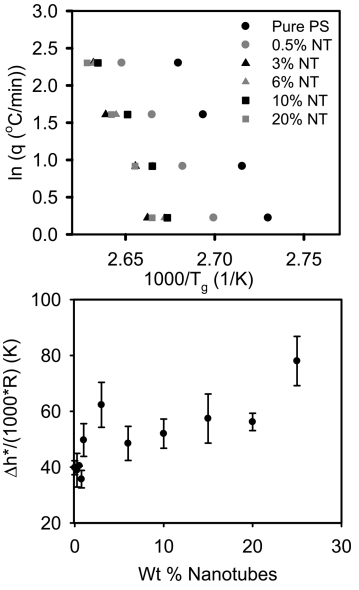

Figure 7. Activation energy as calculated from the change of T_g with cooling rate (eq 2). Error bars represent the standard errors in the best fit lines for the data represented by the top graph. In these experiments, cooling rate = heating rate.

how the SWCNTs affect polymer dynamics. Before describing the results of these different analyses, it should be emphasized that the change in the heat capacity jump indicates that the material participating in the relaxation at the glass transition is different for different samples. Hence, a particular thermal measurement may be affected by some or all of the material that is not part of the heat capacity jump, and another measurement may not be affected at all by this material. This observation is made because the measurements of different properties, unfortunately, do not yield a consistent picture and this difference in populations could be the source of that disagreement.

Figure 6 shows how the fictive temperature changes with annealing time (eq 1). Only a limited number of samples are shown in the top graph, so the reader can clearly see that the data does not give a very straight line; the curves have much more of an s-shape. Similar data presented by Nutt et al.[6] as well as that of Simon et al.[48] showed some s-shape character as well, but the effect is more pronounced here. As the bottom plot of Figure 6 indicates, the variation in slopes was surprisingly small given how poor a line actually describes the data. The graph on the bottom of Figure 6 is essentially the exact analogue of the behavior shown in Figure 3: a decrease in mobility followed by a plateau. In this case, a decrease in relaxation rate represents a decrease in mobility; while in Figure 3 an increase in T_g represents a decrease in mobility. In the paper by Nutt et al.,[6] T_g and the relaxation rate also trended toward decreasing mobility, although in both cases no plateau was found up to 10 wt % clay.

Figure 7 shows the results of calculation of the activation energy of the glass transition (eq 2). The top plot of the data shows the raw data from which a slope is fit; nonlinearity is not evident over the order of magnitude variation in cooling rate. Such nonlinearity in these types of curves is expected because the glass transition tends to follow a WLF type of relationship, not an Arrhenius one; however nonlinearity is not very evident in a curve for polystyrene presented elsewhere over a cooling range from 5 to 25 °C/min.[49] The general shape of the curve shown in the bottom of Figure 7 is difficult to discern because of the error; the curve appears to be a monotonic increase in activation energy. An increase in activation energy is consistent with an increase in the cooperative motion associated with the glass transition. A previous paper used this same procedure to compare a polystyrene sample and one filled with 10% clay and found a drop in activation energy from a starting value statistically identical the one presented here to one 33% less; the T_g increase was about 10 °C with the addition of 10% clay.[49] However, isoconversion methods detailed in this same paper found a higher activation energy for the nanoclay composite; the author did not explain the source of the discrepancy.

Table 1. Enthalpic Overshoots (J/$g_{polymer}$ °C) when Heating Rate = Cooling Rate[a]

sample	2.5 °C/min	1.25 °C/min
PS	0.22	0.28
0.25% SWCNT	0.11	0.23
0.50% SWCNT	0.15	0.27
0.75% SWCNT	0.18	0.25
1.0% SWCNT	0.23	0.25
3.0% SWCNT	0.23	0.31
6.0% SWCNT	0.20	0.26
10% SWCNT	0.49	0.25
15% SWCNT	0.18	0.36
20% SWCNT	0.26	0.25
25% SWCNT	0.17	0.26

[a] Rates of 5 and 10 °C/min had uniform enthalpic overshoots of 0.

A recent article by Simon et al.[50] suggested that the use of heating curves and isoconversion methods to find the activation energy is flawed because of the substantial enthalpy overshoot. This same comment is relevant to the procedure employed in this paper, since in essence the method used evaluates T_g at ~50% conversion of the C_p from the solid to the liquid. Simon et al. argue that to possibly eliminate this problem, the enthalpic overshoot should be constant for the different rates used for a given sample; such was not the case in our experiments since the enthalpic overshoot increased as the rate got smaller as shown in Table 1, although in all cases the values were rather small. Simon asserts that the manifestation of the kinetic overshoot is that the activation energy is too low. However, the value of the activation energy is not of interest here, rather the change with the introduction of nanotubes. Except for one clear outlier, the enthalpic overshoots were fairly consistent from sample-to-sample.

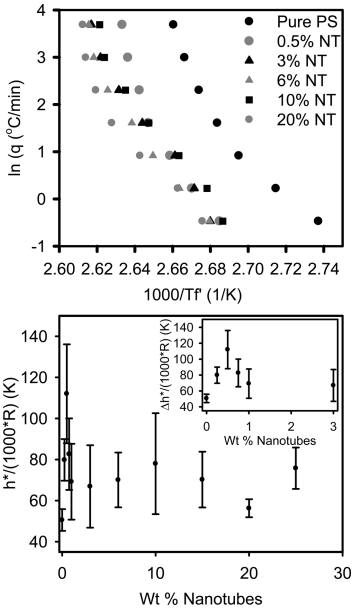

Figure 8. Activation energy calculated from the cooling rate dependence of T_f'. Top represents raw data; in this procedure a line is fit to this obviously curved data. Error bars represent the standard deviation from running multiple trials, which were much larger than those represented by the standard errors of the best-fit line. In these experiments, the cooling rate varied and the heating rate was 10 °C/min.

Hence, it is reasonable to assume that the relative positions of the values shown in the bottom of Figure 7 are not affected by this problem.

Figure 8 shows the activation energy calculated from the limiting fictive temperature (eq 1). For pure polystyrene, this value is on the lower end of activation energies for the glass transition calculated via a variety of techniques.[50] However, the difference between the activation energy calculated using this technique and that from the T_g (Figure 7) is only about 25%, very similar to the percentage difference noted in a previous study.[50] The top plot shows noticeable curvature in the raw data at $>3\%$ nanotubes; the nature of the curvature is consistent with a higher activation energy at higher temperatures which is not consistent with a WLF-type description of the data.

The change in the activation energy with nanotube content is even more surprising. When the change in the heat capacity is falling (Figure 4) the activation energy is significantly larger than that of pure polystyrene; when the amount of nanotubes reaches 1%, the value of the activation energy is only slightly larger than that of pure polystyrene and may not be statistically significantly different. In other words, during the process of formation of a continuous network, there is a significant increase in the activation energy. The fact that there is a decrease at higher nanotube contents is really quite surprising, and could possibly be due to the reduction in the amount of material that is participating in the glass transition. However, if the latter explanation is correct, then the expectation would be that the activation energy would change as the ΔC_p changes at very high nanotube contents, which does not occur. At this point, the source of the unique shape of the bottom of Figure 8 is not understood.

In a previous paper by Lu and Nutt[6] with nanoclay filler, Δh^* increased monotonically with increasing nanofiller content, which was attributed to an increase in the cooperative nature of the glass transition. In other words, the energy barrier required to achieve the configuration rearrangement associated with the increase in enthalpy relaxation is higher. The magnitude of the increase with filler content was about 50% at 10% filler content. In the graphitic nanofiber case,[12] the same type of nonmonotonic behavior seen here was found; although as mentioned previously the weight fractions were much lower so it was not clear whether a constant activation energy was found at higher weight fractions.

Conclusions

Heat capacity measurements indicate that less material participates in the glass transition with added SWCNTs. Various measures were used to assess the effect of nanotube addition on the polymer mobility as measured by the behavior around the glass transition, and in general the results showed a decrease in mobility with the addition of nanotubes. The exact qualitative nature of this decrease, i.e., was the decrease monotonic or was there a plateau, differed for different measurements. This result likely is due to how complicated the system is from a dispersion perspective, since there is no guarantee that the dispersion is the same for different nanotube fraction systems; and from a mobility perspective, since the results indicate a change in the amount of material that participates in the glass transition. Perhaps the most interesting result was that at very high nanotube fractions, there was an increase in the heat capacity change at T_g, likely indicative that nanotubes are participating in the molecular motion that defines the glass transition.

Acknowledgment. This research was supported by grants from the Oklahoma State Regents for Higher Education and the Department of Energy (Grant ER64239 0012293). We would also like to thank the anonymous reviewers that made important contributions to the quality of this paper.

References and Notes

(1) Keddie, J. L.; Jones, R. A. L.; Cory, R. A. *Faraday Disc.* **1994**, *98*, 219–230.
(2) Jones, R. A. L. *Curr. Opin. Colloid Interface Sci.* **1999**, *4*, 153–158.
(3) Hall, D. B.; Torkelson, J. M. *Macromolecules* **1998**, *25*, 8817–8825.
(4) Priestley, R. D.; Ellison, C. J.; Broadbelt, L. J.; Torkelson, J. M. *Science* **2005**, *309*, 456–459.
(5) Bansal, A.; Yang, H. C.; Li, C. Z.; Cho, K. W.; Benicewicz, B. C.; Kumar, S. K.; Schadler, L. S. *Nat. Mater.* **2005**, *4*, 693–698.
(6) Lu, H. B.; Nutt, S. *Macromolecules* **2003**, *36*, 4010–4016.
(7) Chen, K.; Wilkie, C. A.; Vyazovkin, S. *J. Phys. Chem. B* **2007**, *111*, 12685–12692.
(8) Vyazovkin, S.; Dranca, I. *J. Phys. Chem. B* **2004**, *108*, 11981–11987.
(9) Rittigstein, P.; Torkelson, J. M. *J. Polym. Sci., B: Polym. Phys.* **2006**, *44*, 2935–2943.
(10) Ash, B. J.; Siegel, R. W.; Schadler, L. S. *J. Polym. Sci., B: Polym. Phys.* **2004**, *42*, 4371–4383.
(11) Amanuel, S.; Gaudette, A. N.; Sternstein *J. Polym. Sci., B: Polym. Chem.* **2008**, *46*, 2733–2740.
(12) Khojin, A. S.; Jana, S.; Zhong, W. H. K. *J. Mater. Sci.* **2007**, *42*, 6093–6101.
(13) Sargsyan, A.; Tonoyan, A.; Davtyan, S.; Schick, C. *Eur. Polym. J.* **2007**, *43*, 3113–3127.
(14) Yang, Y. K.; Xie, X. L.; Wu, J. G.; Mai, Y. W. *J. Polym. Sci., A: Polym. Chem.* **2006**, *44*, 3869–3881.
(15) Putz, K. W.; Mitchell, C. A.; Krishnamoorti, R.; Green, P. F. *J. Polym. Sci., B: Polym. Phys.* **2004**, *42*, 2286–2293.
(16) Miaudet, P.; Derre, A.; Maugey, M.; Zakri, C.; Piccione, P. M.; Inoubli, R.; Poulin, P. *Science* **2007**, *5854*, 1294–1296.
(17) Jin, S. H.; Choi, D. K.; Lee, D. S. *Colloid Surf. A* **2008**, *313*, 242–245.
(18) Ha, M. L. P.; Grady, B. P.; Lolli, G.; Resasco, D. E.; Ford, W. T. *Macromol. Chem. Phys.* **2007**, *208*, 446–456.
(19) Xia, H.; Song, M. *J. Mater. Chem.* **2006**, *16*, 1843–1851.
(20) Shieh, Y. T.; Liu, G. L. *J. Polym. Sci., B: Polym. Phys.* **2007**, *45*, 1870–1881.
(21) Tchoul, M. N.; Ford, W. T.; Ha, M. L. P.; Chavez-Sumarriva, I.; Grady, B. P.; Lolli, G.; Resasco, D. E.; Arepalli, S. *Chem. Mater.* **2008**, *20*, 3120–3126.
(22) http://athas.prz.rzeszow.pl/.
(23) Badrinarayanan, P.; Zheng, W.; Li, Q.; Simon, S. L. *J. Non-Cryst. Sol.* **2007**, *353*, 2603–2612.
(24) Neuenfeld, S.; Schick, C. *Thermochim. Acta* **2006**, *446*, 55–65.

(25) Tool, A. Q. *J. Am. Ceram. Soc*. **1946**, *29*, 240–242.
(26) Moynihan, C. T.; Easteal, A. J.; De Bolt, M. A.; Tucker, J. *J. Am. Ceram. Soc*. **1976**, *59*, 12–16.
(27) Narayanaswamy, O. S. *J. Am. Ceram. Soc*. **1971**, *54*, 491–497.
(28) Moynihan, C. T.; Easteal, A. J.; Wilder, J. *J. Phys. Chem*. **1974**, *78*, 2673–2677.
(29) Moynihan, C. T.; Lee, S.-K.; Tatsumisago, M.; Minami, T. *Thermochim. Acta* **1996**, *280/281*, 153–162.
(30) Saiter, A.; Couderc, H.; Grenet, J. J. *Therm. Anal. Calor*. **2007**, *88*, 483–488.
(31) Du, F.; Scogna, R. C.; Zhou, W.; Brand, S.; Fischer, J. E.; Winey, K. I. *Macromolecules* **2004**, *37*, 9048–9055.
(32) Grossiord, N.; Miltner, H. E.; Loos, J.; Meuldijk, J.; Van Mele, B.; Koning, C. E. *Chem. Mater*. **2007**, *19*, 3787–3792.
(33) Choi, Y. J.; Hwang, S. H.; Hong, Y. S.; Kim, J. Y.; Ok, C. Y.; Huh, W.; Lee, S. W. *Polym. Bull*. **2005**, *53*, 393–400.
(34) Pham, J. Q.; Mitchell, C. A.; Bahr, J. L.; Tour, J. M.; Krishanamoorti, R.; Green, P. F. *J. Polym. Sci., Part B: Polym. Phys*. **2003**, *41*, 3339–3345.
(35) Shanmugharaj, A. M.; Bae, J. H.; Nayak, R. R.; Ryu, S. H. *J. Polym. Sci., Part A: Polym. Chem*. **2007**, *45*, 460–470.
(36) Cipriano, B. H.; Kota, A. K.; Gershon, A. L.; Laskowski, C. J.; Kashiwagi, T.; Bruck, H. A.; Raghavan, S. R. *Polymer* **2008**, *49*, 4846–4851.
(37) Alig, I.; Lellinger, D.; Dudkin, S. M.; Potschke, P. *Polymer* **2007**, *48*, 1020–1029.
(38) Alig, I.; Skipa, T.; Lellinger, D.; Bierdel, M.; Meyer, H. *Phys. Stat. Solidi B: Basic Solid State Phys*. **2008**, *245*, 2264–2267.
(39) Alig, I.; Lellinger, D.; Engel, M.; Skipa, T.; Pötschke, P. *Polymer* **2008**, *49*, 1902–1909.
(40) Alig, I.; Skipa, T.; Engel, M.; Lellinger, D.; Pegel, S.; Pötschke, P. *Phys. Stat. Solidi B: Basic Solid State Phys*. **2007**, *244*, 4223–4226.
(41) Alig, I.; Skipa, T.; Lellinger, D.; Engel, M.; Pötschke, P. *Polymer* **2008**, *49*, 3524–3532.
(42) Traina, M.; Pegoretti, A.; Penati, A. *J. Appl. Polym. Sci*. **2007**, *106*, 2065–2074.
(43) Heinrich, G.; Costa, F. R.; Abdel-Goad, M.; Wagenknecht, U.; Lauke, B.; Hartel, V.; Tschimmel, J.; Kluppel, M.; Svistkov, A. L. *Kautsch. Gummi Kunst*. **2005**, *58*, 163–167.
(44) Zhang, C.; Wang, P.; Ma, C. A.; Wu, G. Z.; Sumita, M. *Polymer* **2006**, *47*, 466–473.
(45) Chae, H. G.; Minus, M. L.; Kumar, S. *Polymer* **2006**, *47*, 3494–3504.
(46) O'Connell, M. J.; Boul, P.; Ericson, L. M.; Huffman, C.; Wang, Y.; Haroz, E.; Kuper, C.; Tour, J.; Ausman, K. D.; Smalley, R. E. *Chem. Phys. Lett*. **2001**, *342*, 265–271.
(47) Peters, J. E.; Papavassiliou, D. V.; Grady, B. P. *Macromolecules* **2008**, *41*, 7274–7277.
(48) Koh, Y. P.; Simon, S. L. *J. Polym. Sci., B: Polym. Chem*. **2008**, *46*, 2741–2753.
(49) Vyazovkin, S.; Dranca, I. *J. Phys. Chem. B* **2004**, *108*, 11981–11987.
(50) Badrinarayanan, P.; Zheng, W.; Simon, S. L. *Thermochim. Acta* **2008**, *468*, 87–93.